



UNIVERSITY  
OF TRENTO

---

**DIPARTIMENTO DI INGEGNERIA E SCIENZA DELL'INFORMAZIONE**

---

38123 Povo – Trento (Italy), Via Sommarive 14  
<http://www.disi.unitn.it>

GA-ENHANCED ADS-BASED APPROACH FOR ARRAY  
THINNING

G. Oliveri, and A. Massa

January 2011

Technical Report # DISI-11-106



# **GA-Enhanced ADS-Based Approach for Array Thinning**

G. Oliveri and A. Massa

*ELEDIA Research Group*

Department of Information and Communication Technologies,

University of Trento, Via Sommarive 14, 38050 Trento - Italy

Tel. +39 0461 882057, Fax +39 0461 882093

E-mail: *andrea.massa@ing.unitn.it*, *giacomo.oliveri@dit.unitn.it*

Web-site: *http://www.eledia.ing.unitn.it*

# GA-Enhanced ADS-Based Approach for Array Thinning

G. Oliveri and A. Massa

## Abstract

This paper proposes a Genetic Algorithm (*GA*)-enhanced Almost Difference Set (*ADS*)-based methodology to design thinned linear arrays with low peak sidelobe levels (*PSLs*). The method allows one to overcome the limitations of the standard *ADS* approach in terms of flexibility and performances. The numerical validation, carried out in the far-field and for narrow-band signals, points out that with affordable computational efforts it is possible to design array arrangements that outperform standard *ADS*-based designs as well as standard *GA* approaches.

**Key words** - Array Antennas, Linear Arrays, Thinned Arrays, Almost Difference Sets, Sidelobe Control.

# 1 Introduction

Modern radars for remote sensing and traffic control, devices for satellite and ground communications, and biomedical imaging systems often require radiation patterns with a very high directivity [1]. To meet this requirement, large thinned arrays are usually used because of their advantages in terms of weight, consumption, hardware complexity, and costs over their filled counterparts [1]. Unfortunately, thinning large arrays reduces the control of the peak sidelobe level (*PSL*). In order to overcome such a limitation, several techniques have been proposed (e.g., random techniques [2][3], algorithmic approaches [3], dynamic programming [4], genetic algorithms [5][6], simulated annealing [7][8], and particle swarm optimizers [9]) and efficient methods for designing thinned arrays with low *PSL*s are still of great interest [10] due to their importance in practical applications [11]. Difference Sets (*DS*s) have been at first employed to analytically determine thinned arrangements with well controlled sidelobes [10]. More recently, such an analytical approach has been extended to a wider class of geometries by exploiting the mathematical properties of Almost Difference Sets (*ADS*s) [12][13]. Reliable and *a-priori* predictable bounds for the *PSL* of the synthesized arrays have been provided [14], as well. Moreover, the reliability of the analytic *ADS*-based thinning has been analyzed also taking into account the mutual coupling effects among array elements [16]. However, despite several interesting features and advantages, the use of *ADS* sequences for array thinning has some limitations that could prevent their widespread exploitation in real applications [14][16]. More specifically:

1. *ADS*-based arrays usually provide sub-optimal *PSL* performances;
2. although large repositories of *ADS*s are available [17], *ADS* arrays with arbitrary aperture sizes and thinning factors cannot be designed, since *ADS* sequences exist only for specific sets of descriptive parameters;
3. even for admissible aperture sizes and thinning factors, general purpose *ADS* construction techniques do not exist at present and the explicit forms of *ADS* sequences has to be determined on a case by case basis using suitable construction theorems [12][13].

This paper is then aimed at introducing a technique able to enhance the *ADS*-based design methodology and to overcome the above limitations. Towards this end, a *GA*-based procedure exploiting and improving the approach in [14] seems to be a potential candidate since: (a) *GAs* are intrinsically able to deal with discrete or binary optimization problems [6] as those of interest, (b) *GAs* have been extensively and successfully applied to array thinning [5], (c) *a-priori* information and constraints from *ADS*-based designs can be easily integrated into the *GA*-based optimization [6]. Accordingly, a *GA*-enhanced *ADS* methodology is hereinafter proposed. Unlike previously published works exploiting *ADS* for thinning [14][16] as well as for other array design problems (such as interleaved arrays [15]), the proposed approach does not rely on a purely analytic technique and, therefore, it does not allow one to determine *a-priori* performance bounds. The main objective of the paper is not only to propose a hybrid technique to design linear thinned arrays, but rather to present a methodological approach useful when/where either the *ADS*-based array performances do not comply with the radiation requirements of the application at hand or no *ADS* is available for the geometry (aperture size or thinning factor) under study. In order to focus on that, the proposed method is applied to three different classes of problems related to the main limitations of *ADS*-based arrays.

The outline of the paper is as follows. After a short review on *ADS* thinning, the *GA*-enhanced methodology is proposed to address three different problems concerned with *ADS*-based linear arrays working in the far-field and with narrowband signals (Sect. 2). The hybrid approach is then validated by means of several numerical simulations. Representative results concerned with both small and large arrays as well as different thinning factors are discussed to point out its reliability (Sect. 3). Finally, some conclusions are drawn (Sect. 4).

## 2 Problem Statement and Mathematical Formulation

The design of an equally-weighted thinned linear array defined over a regularly-spaced lattice of  $N$  elements is carried out by properly selecting the array weights  $w(n) \in \{0, 1\}$ ,  $n = 1, \dots, N$ , to obtain a suitable array factor  $S(u)$  [1]

$$S(u) = \sum_{n=0}^{N-1} w(n) \exp(i2\pi n d u) \quad (1)$$

( $d$  being the inter-element distance in wavelength). According to the *ADS*-based methodology described in [14], the weight selection is performed as follows

$$w(n) = \begin{cases} 1 & \text{if } n \in \mathbf{D} \\ 0 & \text{otherwise} \end{cases}$$

where  $\mathbf{D}$  is an  $(N, K, \Lambda, t)$ -Almost Difference Sets (*ADS*), that is a set of  $K$  unique integers belonging to the range  $[0, N - 1]$ , whose associated binary sequence has a cyclic autocorrelation function,  $\xi(\tau) \triangleq \sum_{n=0}^{N-1} w(n)w[(n + \tau) \bmod N]$ ,  $\tau = 0, \dots, N - 1$ , of period  $N$  given by

$$\xi(\tau) = \begin{cases} K & \tau = 0 \\ \Lambda & \text{for } t \text{ values of } \tau \\ \Lambda + 1 & \text{otherwise.} \end{cases} \quad (2)$$

Because of (2) and the relationship between the autocorrelation function and  $S(u)$ , it results that the samples of the array power pattern at  $\frac{k}{dN}$  are equal to the values of the inverse discrete Fourier transform (*IDFT*) of  $\xi(\tau)$ ,  $\Xi(k) \triangleq \sum_{\tau=0}^{N-1} \xi(\tau) \exp(2\pi i \frac{\tau k}{N})$  [i.e.,  $\Xi(k) = |S(\frac{k}{dN})|^2$ ]. Thanks to this property, it can be shown [14] that the arising *PSL* complies with the following inequality

$$PSL_{MIN}^{opt} \leq PSL_{DW}^{opt} \leq PSL^{opt} \{\mathbf{D}\} \leq PSL_{UP}^{opt} \leq PSL_{MAX}^{opt} \quad (3)$$

where  $PSL^{opt} \{\mathbf{D}\} = \min_{\sigma \in [0, N-1]} \{PSL(\mathbf{D}^{(\sigma)})\}$ ,  $\mathbf{D}^{(\sigma)} \triangleq \{d_k^{(\sigma)} \in \mathbb{Z}^N, k = 1, \dots, K : d_k^{(\sigma)} = (d_k + \sigma) \bmod N\}$  is the  $\sigma$ -shifted version of the original *ADS* ( $\mathbf{D}^{(\sigma)}$  is still an *ADS* [12]),  $PSL(\mathbf{D}^{(\sigma)}) \triangleq \frac{\max_{u \notin R} |S(u)|^2}{|S(0)|^2}$  is the *PSL* of the array deduced by  $\mathbf{D}^{(\sigma)}$ ,  $R \triangleq \{-U \leq u \leq U, U = \frac{1}{2Nd \sqrt{\frac{\max_k \Xi(k)}{\Xi(0)}}}\}$ ,

and the performance bounds are the following:  $PSL_{MIN}^{opt} = \frac{K - \Lambda - 1 - \sqrt{\frac{t(N-t)}{(N-1)}}}{(N-1)\Lambda + K - 1 + N - t}$ ,  $PSL_{DW}^{opt} = \frac{\max_k \Xi(k)}{\Xi(0)}$ ,  $PSL_{UP}^{opt} = \frac{\max_k \Xi(k)}{\Xi(0)} (0.8488 + 1.128 \log_{10} N)$ , and  $PSL_{MAX}^{opt} = \frac{(K - \Lambda - 1 + \sqrt{t(N-t)})}{(N-1)\Lambda + K - 1 + N - t} (0.8488 + 1.128 \log_{10} N)$  [14]. Equation (3) indicates that *ADS*-based thinned arrays exhibit a

sidelobe level which can be predicted *a-priori* either from the knowledge of the features of the *ADS* sequence ( $PSL_{MIN}^{opt}$  and  $PSL_{MAX}^{opt}$  only depend on  $N$ ,  $K$ ,  $\Lambda$ , and  $t$ ) or, with a higher accuracy, from the expression of  $\Xi(k)$  (necessary for computing  $PSL_{DW}^{opt}$  and  $PSL_{UP}^{opt}$ ). Despite the implicit advantages in terms of computational efficiency and predictable performances, the *ADS*-based approach for array thinning has the limitations outlined in the Introduction (Sect. 1). Therefore, a methodology able to overcome these limitations while exploiting the *ADS* analytic features seems to be of some interest in view of its application to wireless communications.

Towards this end, a hybrid approach (*ADSGA* in the following) is proposed. By sake of clarity, the critical situations of the *ADS* approach are modeled in the following sub-sections as suitable optimization problems then solved through the *ADSGA*. Concerning the iterative *ADSGA* optimization, the standard structure of the *GA* (summarized in Appendix I) is modified to exploit the positive key-features of the *ADS*s.

The initial population ( $i = 0$ ,  $i$  being the iteration index) is generated as follows. The  $N$  shifted versions of a reference *ADS* are ranked according to their *PSL* values. Then, half trial solutions ( $P$  being the dimension of the *GA* population) are chosen with chromosomes equal to the binary sequences of the first  $\frac{P}{2}$  highly-ranked shifted *ADS*s

$$\rho_p(i) = \{b_p(n) = w^{(p)}(n); n = 0, \dots, N - 1\}, \quad 1 \leq p \leq \frac{P}{2} \quad (4)$$

where  $b_p(n)$  is the  $n$ -th digit of the  $p$ -th trial solution and  $w^{(\sigma)}(n) = 1$  if  $n \in \mathbf{D}^{(\sigma)}$  and  $w^{(\sigma)}(n) = 0$ , otherwise. Concerning the remaining of the population, the trial solutions are chosen randomly within the range of admissibility of the problem at hand

$$\rho_p(i) = \{b_p(n) = r_p(n); n = 0, \dots, N - 1\}, \quad 1 \leq p \leq \frac{P}{2} \quad (5)$$

$r_p(n)$  being a random digit. Such an initialization allows the “transfer” into the *GA* chromosomes of the good *ADS*-based schemata also providing a sufficient variability within the population to avoid the stagnation [6].

As regards the *GA* operators, both crossover and mutation are applied following the standard

binary implementations [6], but also guaranteeing the updated trial solutions be admissible and comply with the problem constraints (e.g., fixed thinning factor  $\nu \triangleq \frac{K}{N}$ ). Towards this end, the crossover operation is repeated until the new chromosomes satisfy the solution constraints, while a conditioned-mutation is applied. More specifically, let  $\nu$  be the user-defined thinning factor, then the bit-mutation probability is defined as follows

$$P_{BM}(n) = \frac{[N \times \nu - \sum_{m=0}^{n-1} b(m)]}{N - n} \times [1 - 2b(n)] + b(n) \quad (6)$$

## 2.1 Problem I - PSL Minimization in Array Synthesis

In order to determine an optimal thinned configuration starting from the (usually) sub-optimal *ADS* arrangement with a given aperture size  $N_{ADS}$  and thinning factor  $\nu_{ADS}$ , let us formulate the following constrained optimization problem

*Problem I* - Minimize  $F\{\rho\} \triangleq \frac{\max_{u \notin R_M} \{|S(u)|^2\}}{|S(0)|^2}$ ,  $R_M$  being the mainlobe region defined as  $R_M \triangleq \{-U_M \leq u \leq U_M\}$  and  $U_M$  is the angular location of the first null, subject to  $K = K_{ADS}$  and  $N = N_{ADS}$

to be solved through *ADSGA*. In such a case, the *GA* fitness function is defined as the *PSL* of the array while the constraints force the array to keep its descriptive parameters (i.e., original dimension,  $N = N_{ADS}$ , and thinning,  $\nu = \nu_{ADS}$ ).

## 2.2 Problem II - Extension of the Range of ADS Applicability in Array Synthesis

The use of an *ADS*-based technique for array synthesis is sometimes limited to fixed array dimensions and thinning values because of the limited, although quite large, set of available *ADS* sequences. In order to design a thinned configuration with arbitrary values of  $N$  and  $\nu$ , still exploiting the properties of the existing *ADS* arrangements, the following problem is at hand

*Problem II* - Minimize  $F\{\rho\} = \frac{\max_{u \in R_M} \{|S(u)|^2\}}{|S(0)|^2}$  subject to  $K = \hat{K}$  and  $N = \hat{N}$ ,  
being  $\hat{N} \neq N_{ADS}$  and/or  $\hat{K} \neq K_{ADS}$

Such a constrained optimization problem is quite similar to that in Sect. 2.1, but, in this case, no *ADS*-based array is available in correspondence with the array parameters  $(\hat{N}, \hat{K})$ .

### 2.3 *Problem III* - Definition of a General Purpose *ADS* Construction Technique for Array Synthesis

With reference to the potential limitation (III) outlined in the Introduction, the aim is now to find the explicit forms of *ADS*s sequences (i.e., binary sequences with a three-level autocorrelation function) for arbitrary values of  $N$ . Towards this end, let us denote with  $L\{\rho\}$  and  $R\{\rho\}$  the number of levels of the autocorrelation function  $\xi(\tau)$  of a trial solution  $\rho$  and the number of  $\tau$  values for which  $\xi(\tau)$  differ from (2). Then, the search for admissible (but not available in *ADS* repositories) *ADS* sequences is recast as the solution of the following

*Problem III* - Minimize  $F\{\rho\} = \alpha [L\{\rho\} - 3] + \beta R\{\rho\}$  subject to  $N = \hat{N}$ , where  $\hat{N} \neq N_{ADS}$  and  $\alpha$  and  $\beta$  are suitable user-defined weight coefficients.

In such a case, the optimization at hand turns out to be different from that in *Problem I* and *Problem II*. As a matter of fact, it is defined and performed with the *ADSGA* within the “auto-correlation space” instead of in the “pattern space”, while the constraints are still on the set of parameters defining the *ADS* as well as the corresponding array arrangement.

## 3 Numerical Analysis

In this section, the effectiveness of the *ADSGA* in solving Problems I-III is analyzed by discussing a set of representative numerical results concerned with different aperture sizes and thinning factors. The set of parameters of the *GA*-based procedure are:  $P_C = 0.9$  (*crossover rate*),  $P_M = 0.01$  (*mutation rate*), and  $P = N$  (*population size*) if not otherwise stated.

### 3.1 Application to Problem I

The first experiment deals with the (100, 50, 24, 25)-ADS [17] ( $N_{ADS} = 100$ ,  $\nu_{ADS} = 0.5$ ).

Figure 1(a) shows the behavior of the optimal fitness value

$$F_{POP}(i) = \min_p [F \{\rho_p(i)\}], \quad p = 0, \dots, P - 1, \quad (7)$$

versus the iteration number  $i$  in correspondence with the *ADSGA* and the standard *GA* minimization ( $d = \frac{1}{2}$  is assumed hereinafter). The *PSL* value of the reference *ADS* sequence is reported, as well. Obviously,  $F_{POP}^{ADS}(0) \leq F_{POP}^{ADSGA}(0)$  since the *ADS* sequence belongs to the initial population of the *ADSGA*. It is also worth to notice that the convergence<sup>(1)</sup> rate of the optimization process improves when using the *ADSGA* as compared to the *GA*-bare approach (while the average iteration time<sup>(2)</sup> does not sensibly change - Tab. I). As a matter of fact,  $I^{ADSGA} = 386$  iterations are necessary to reach the convergence, while  $I^{GA} = 598$  [ $I_{max} = 1000$  - Fig. 1(a)]. Moreover, the thinned arrangement synthesized with *ADSGA* turns out to be significantly better than the reference *ADS* in terms of *PSL* [ $PSL^{ADSGA} = -20.64$  dB vs.  $PSL^{ADS} = -14.45$  dB]. Furthermore, it improves the performance of the *GA* of about 1 dB as confirmed by the plots of the corresponding power patterns [Fig. 1(c)].

However, both *GA*-based optimizations also enlarge the mainlobe beamwidth compared to the *ADS* reference solution [ $U_M^{ADSGA} \approx U_M^{GA} = 0.041$  vs.  $U_M^{ADS} = 0.020$  - Tab. I] because of the quasi-dense nature of the arising layouts (in both cases, the average spacing is close to  $0.6\lambda$  - Tab. I). In order to perform a more fair comparison, another optimization has been carried out by setting a constraint on the extension of  $R_M$ , as well. More specifically, the mainlobe region has been required to be equal to that of the “best” *ADS*-based array, that is the shifted array with the best trade-off between *PSL* and  $R_M$  among all *ADS* layouts whose representative points belong to the Pareto front (i.e., the set of all nondominated solutions [6]) in the (*PSL*,  $R_M$ ) plane (Fig. 2):  $R_M = R_M^{ADS}$ . The obtained results are shown in Figs.

<sup>(1)</sup> The process is assumed to *converge* when the fittest (within  $I_{max}$  iterations) solution  $\rho_{conv}$  has been reached. Accordingly,  $I$  ( $I \leq I_{max}$ ) is the “convergence iteration” such that  $F \{\rho_{conv}\} = (\min_p [F \{\rho_p(I)\}]) = \min_i (\min_p [F \{\rho_p(i)\}])$ .

<sup>(2)</sup> The values of the *average iteration time* have been computed by exploiting non-optimized *C*-coded versions running on an Intel 2.1 GHz single core laptop.

1(b)-1(d)-1(f). As expected, the *PSL* improvement of the *ADSGA* over the *ADS* turns out to be smaller, although non-negligible [ $PSL_C^{ADSGA} = -16.39$  - Fig. 1(d)], and the number of iterations to reach the final design increases ( $I_C^{ADSGA} = 629$  vs.  $I^{ADSGA} = 704$ ). On the other hand and unlike the unconstrained case [Fig. 1(e)], the array elements of the new arrangements [Fig. 1(f)] are now distributed within a spatial range  $\Phi$  of extension close to that of  $\Phi^{ADS}$  (i.e.,  $\Phi_C^{ADSGA} = 45.5 \lambda$ ,  $\Phi_C^{GA} = 44.5 \lambda$ , and  $\Phi^{ADS} = 48.5 \lambda$ ) in order to fit the beamwidth condition  $R_M = R_M^{ADS}$ .

Similar conclusions generally hold true also for wider apertures as confirmed by the resuming plots in Fig. 3 where the values of the *PSL* [Fig. 3(a)] and the mainlobe size  $U_M$  [Fig. 3(b)] along with the behavior of  $I_{conv}$  [Fig. 3(c)] and of the normalized aperture  $\frac{\Phi}{N}$  [Fig. 3(d)] are reported as functions of the array size  $N$  for both the  $R_M$ -constrained and unconstrained problems. With reference to Fig. 3(a), the *ADSGA* provides enhanced performances in comparison with the *GA* for any array size  $N$ , even though the improvements are not always very significant. Furthermore, both *GA*-based techniques result better than the reference *ADS* arrangements, setting or not the same mainlobe beamwidth. As expected, the improvements of the  $R_M$ -constrained synthesis are lower, but the differences with the unconstrained approach reduce as  $N$  grows since  $\Phi_C \rightarrow \Phi$  [Fig. 3(d)] and  $U_M^C \rightarrow U_M$  [Fig. 3(b)]. On the other hand, the plots in Fig. 3(c) point out the following: (i) the iteration index  $I_{conv}$  increases dealing with a higher complexity problem (i.e.,  $R_M$ -constrained vs.  $R_M$ -unconstrained) or a larger solution space ( $S = 2^N$ ,  $S$  being the dimension of the solution space as a function of the array lattice dimension); (ii) whatever the dimension and the synthesis,  $I_{conv}^{ADSGA} \leq I_{conv}^{GA}$  thanks to the *ADS* initialization and the customized genetic evolution of the *ADSGA* optimization.

For illustrative purposes, Figures 4-5 and Tabs. II-III complete the “picture” coming from Fig. 1 and concerned with a small arrangement ( $N = 100$ ) with those on the synthesis of a medium array ( $N = 198$  - Fig. 4 and Tab. II) and a large array ( $N = 502$  - Fig. 5 and Tab. III). More specifically, the power patterns and the corresponding arrangements generated from the (198, 99, 49, 148)-*ADS* [17] ( $\nu_{ADS} \approx 0.5$ ) are reported in Fig. 4, while the case of the (502, 251, 125, 376)-*ADS* [17] ( $\nu_{ADS} \approx 0.5$ ) is analyzed in Fig. 5.

### 3.2 Application to Problem II

Dealing with the application of the *ADSGA* to Problem II, let us consider the (198, 99, 49, 148)-*ADS* [17] ( $\nu_{ADS} \approx 0.5$ ) and let us set the following objective parameters:  $\hat{N} = 198$ ,  $\hat{\nu} = 0.601$ , and  $I_{max} = 2000$ . It is worthwhile to note that the thinning factor of the reference *ADS* and of the initial population differ from that of the target array.

The plots in the first row of Fig. 6 show the evolution of the fitness function during the iterative process for the approaches with and without the constraint on  $R_M$ . Also in this case, the *ADSGA* enhances the optimization performances of the standard *GA* approach [Fig. 6(a)-6(b)] synthesizing the power patterns shown in Figs. 6(c)-6(d) whose characteristics are summarized in Tab. IV. More in detail, the *PSL* of the optimal  $R_M$ -unconstrained *ADSGA* (*GA*) configuration is of about 4 dB lower than that of the *ADS* [Fig. 6(a) - Tab. IV]. Such an enhancement is also kept almost unaltered when matching the mainbeam width requirement. On the other hand and as expected, it should be pointed out that the amount of the *PSL* improvement turns out to be more significant than for the similar test case of the Problem I because of the larger number of active elements ( $\hat{\nu} = 0.601$  vs.  $\nu = 0.5$ ) in the array [Fig. 6(c)].

To further validate the proposed approach, Problem II has been re-formulated by using again the (198, 99, 49, 148)-*ADS* [17] ( $\nu_{ADS} \approx 0.5$ ) as the reference, but now setting  $\hat{N} = 200$  and  $\hat{\nu} = 0.77$  (i.e., a target array with both different dimension and thinning factor). Such a parameter setup has been chosen to compare the synthesized solution with those from state-of-the-art *GA* optimizations available in the literature [5][6]. Since the pattern in [5] presents a beamwidth different from  $R_M^{ADS}$  ( $U_M^{[Haupt\ 1994]} = 0.0125$  vs.  $U_M^{ADS} = 0.0108$ ), the results from the  $R_M$ -unconstrained problem are at first analyzed.

The *ADSGA* solution is characterized by a fitness value at  $I_{conv} = 1598$  ( $I_{max} = 3000$ ) of almost 7 dB below that obtained with the reference *ADS* [Fig. 7(a) - Tab. V]. Such a non-negligible improvement is mainly due to the increased aperture size ( $N = 200$  vs.  $N^{ADS} = 198$ ) and to the larger number of active elements ( $K = 144$  vs.  $K^{ADS} = 99$ ) [Fig. 7(c)]. On the other hand, by comparing the *ADSGA* result with that from the standard *GA* approach and the state-of-the-art *GA* in [5], the *ADSGA* improvement is of about 0.6 dB and 1 dB, respectively [Fig. 7(b)]. It is worth noting that this reduction is certainly related to the *ADS*

initialization and it is obtained without enlarging the mainlobe region ( $U_M^{[Haupt1994]} = 0.0125 \approx U_M^{ADSGA} = 0.0120$ ). The arrangements in correspondence with the difference solutions are provided in Fig. 7(c).

Dealing with the same test case, but constraining the array to fit the *ADS* beamwidth, the *ADSGA* method confirms its reliability and efficiency synthesizing an array with performances, summarized in Tab. V, close to that of the unconstrained solution and still better than those in [5] (Fig. 8).

For completeness, Figure 8 provides an overview of the results concerned with Problem II. As it can be noticed, the *ADSGA* solution overcomes the *GA*-based designs whatever the test case at hand further pointing out the convenience of the *ADS* initialization and its integration with the *GA* optimization.

### 3.3 Application to Problem III

To complete the preliminary validation presented in [18] (but there limited to the use of a 'bare' *GA* procedure) and to further confirm, in a more exhaustive fashion, the underlying proof-of-concept, a representative example of the numerical definition of new *ADS* sequences is performed by choosing  $\hat{N} = 55$  (nor *ADS* sequence with such a length is known/available [17], neither suitable theorems for its computation are available). The *GA* parameters have been set to:  $I_{max} = 50$ ,  $\alpha = 10^{-2}$ ,  $\beta = 10^{-4}$ . Moreover, the (53, 14, 3, 26)-*ADS* [17] has been assumed as the starting point for the optimization process.

The plot of the optimal fitness in Fig. 9(a) shows that an *ADS* of the desired size has been found just after  $I_{conv} = 34$  iterations [ $F_{POP}(I_{conv}) = 0$ ] as confirmed by the three-level autocorrelation function of the arising optimal sequence [Fig. 9(b)]. As it can be observed, the synthesized *ADS* is characterized by  $K = 7$  ( $K \triangleq \max_{\tau} \{\xi(\tau)\}$ ),  $\Lambda = 0$  ( $\Lambda \triangleq \min_{\tau} \{\xi(\tau)\}$ ), and  $t = 12$  [ $t$  being the number of  $\tau$  values for which  $\xi(\tau) = \Lambda$ ]. For completeness, the binary arrangement is given in Fig. 9(c).

Similar results can be also obtained for larger  $\hat{N}$  values, even though with a greater number of iterations, assessing the reliability of the approach whatever the dimension at hand. For illustrative purposes, a different instance of the Problem III is addressed by setting  $\hat{N} = 214$

(once again, no explicit expression for the corresponding *ADS* is available [17]). Because of the wider solution space, the maximum number of iterations has been enlarged to  $I_{max} = 1500$ , while keeping the same values of the other parameters. Moreover, the following reference *ADS* has been chosen: (210, 105, 52, 157)-*ADS* [17].

As expected, the optimal sequence has been synthesized after more than 1200 iterations [Fig. 10(a)] with a significant increase of the computational cost for reaching the convergence compared to the previous smaller case. Anyway, the approach is still able to define a binary configuration [Fig. 10(c)] with three-levels [Fig. 10(b)] as requested for the *ADS* sequences. More specifically, the new *ADS* is described by the following parameters:  $K = 10$ ,  $\Lambda = 0$ , and  $t = 123$ .

As a final observation, it is worthwhile to point out that the new *ADS*s determined solving different instances of Problem III can be directly used to define new thinned arrays or as starting points for different formulations of Problem I or Problem II. Indeed, the power patterns  $|S(u)|^2$  of the arrays derived from the binary sequences (55, 7, 0, 12)-*ADS* [Fig. 11(a)] and (214, 10, 0, 123)-*ADS* [Fig. 11(b)] fit the *ADS* radiation properties with samples constrained to the associated  $\Xi(k)$  values.

## 4 Conclusions and Remarks

In this paper, a hybrid *GA*-based approach has been developed to further exploit and enhance the features in the far-field and for narrow-band signals of *ADS*-based binary sequences for linear array thinning. In order to overcome the main limitations (i.e., flexibility and performances) of *ADS*-based thinned arrays, while taking advantage of their properties, an innovative methodological approach that, unlike the *ADS* thinning techniques described in [14], does not rely on purely analytical design method, has been proposed.

An extensive numerical analysis has been performed by addressing different kinds of problems, each one concerned with a specific *ADS* limitation. The obtained results have pointed out the following outcomes:

- thanks to the *ADS* initialization, the *ADSGA* provides improved performances with

respect to a standard *GA* approach when dealing with linear array thinning, even though the improvements are not always very significant;

- *ADSGA*-constrained designs are usually advantageous since they avoid both quasi-dense layouts of limited practical importance as well as large mainlobe widths, unlike unconstrained architectures;
- the knowledge of *ADS* reference sequences and the *a-priori* information on the performances of the corresponding arrays turn out to be useful even for synthesizing antenna arrangements with different (also when *ADS*s do not exist) thinning factors or sizes;
- the hybrid approach can be profitably employed to determine the explicit form of new *ADS* sequences of desired length beyond those already available [17], thus extending the range of applicability of the *ADS*-based array thinning.

As regards the array synthesis, future developments will be aimed at assessing the performances of the hybrid approach in dealing with non-ideal structures (e.g., mutual coupling effects and real radiators). Moreover, extensions to more complex and high-dimension array geometries will be analyzed to verify advantages and potentialities, but also limitations and reliability, of the *ADSGA* approach in terms of radiation properties and implementation/HW issues.

## Appendix I

In this section, the building blocks of the *GA* considered in this paper are briefly summarized.

1. **Initialization** - A randomly-chosen initial ( $i = 0$ ) population of  $P$  trial solutions,  $\rho_p(i)$ ,  $p = 1, \dots, P$  is defined;
2. **Coding** - Each solution  $\rho_p(i)$  (*individual*) codes the values of an unknown set of parameters into a binary string (*chromosome*);
3. **GA-Evolution** - At each iteration  $i$ , the genetic evolution takes places through suitable binary operators (*selection, crossover, reproduction, mutation, elitism* [9][6]) applied in

a probabilistic fashion and taking into account the fitness values  $F_p = F\{\rho_p(i)\}$ ,  $p = 1, \dots, P$  of current trial solutions;

4. **Termination** - The iterative optimization terminates when the optimal fitness value,  $F_{POP}(i) = \min_p \{F_p\}$ , is smaller than a user-defined threshold or when a maximum number of iterations  $I_{max}$  has been reached. The “*final solution*” is the fittest trial solution determined throughout the whole iterative process,  $\rho_{conv} = \arg \{ \min_i (\min_p [F\{\rho_p(i)\}]) \}$ .

## References

- [1] Balanis C. A., “Antenna Theory: Analysis and Design” (John Wiley and Sons, New Jersey, 1997) (Second edition)
- [2] Lo Y. T., “A mathematical theory of antenna arrays with randomly spaced elements,” *IEEE Trans. Antennas Propag.*, 1964, **12**, (3), pp. 257-268
- [3] Steinberg B., “Comparison between the peak sidelobe of the random array and algorithmically designed aperiodic arrays,” *IEEE Trans. Antennas Propag.*, 1973, **21**, (3), pp. 366-370
- [4] Holm S., Elgetun B., and Dahl G., “Properties of the beampattern of weight- and layout-optimized sparse arrays,” *IEEE Trans. Ultrason., Ferroelectr., Freq. Control*, 1997, **44**, (5), pp. 983-991
- [5] Haupt R. L., “Thinned arrays using genetic algorithms,” *IEEE Trans. Antennas Propag.*, 1994, **42**, (7), pp. 993-999
- [6] Haupt R. L. and Werner D. H., “Genetic algorithms in electromagnetics” (John Wiley and Sons, New Jersey, 2007)
- [7] Trucco A. and Murino V., “Stochastic optimization of linear sparse arrays,” *IEEE J. Ocean Eng.*, 1999, **24**, (3), pp. 291-299
- [8] Trucco A., “Weighting and thinning wide-band arrays by simulated annealing,” *Ultrasonics*, 2002, **40**, (1-8), pp. 485-489

- [9] Caorsi S., Lommi A., Massa A., and Pastorino M., "Peak sidelobe reduction with a hybrid approach based on GAs and difference sets," *IEEE Trans. Antennas Propag.*, 2004, **52**, (4), pp. 1116-1121
- [10] Leeper D. G. , "Isophoric arrays - massively thinned phased arrays with well-controlled sidelobes," *IEEE Trans. Antennas Propag.*, 1999, **47**, (12), pp. 1825-1835
- [11] Mailloux R. J. , "Phased Array Antenna Handbook", (Artech House, Boston, 2005) (Second edition).
- [12] Ding C., Helleseth T., and Lam K. Y., "Several classes of binary sequences with three-level autocorrelation," *IEEE Trans. Inf. Theory*, 1999, **45**, (7), pp. 2606-2612
- [13] Arasu K. T., Ding C., Helleseth T., Kumar P. V., and Martinsen H. M., "Almost difference sets and their sequences with optimal autocorrelation," *IEEE Trans. Inf. Theory*, 2001, **47**, (7), pp. 2934-2943
- [14] Oliveri G., Donelli M., and Massa A., "Linear array thinning exploiting almost difference sets," *IEEE Trans. Antennas Propag.*, 2009, **58**, (12), pp. 3800-3812
- [15] Oliveri G. and Massa A., "Fully interleaved linear arrays with predictable sidelobes exploiting almost difference sets," *IET Radar, Sonar & Navigation*, (*in press*)
- [16] Oliveri, G., Manica L., and Massa A., "On the impact of mutual coupling effects on the PSL performances of ADS thinned arrays," *Progress In Electromagnetics Research B*, 2009, **17**, pp. 293-308
- [17] ELEDIA Almost Difference Set Repository (<http://www.eledia.ing.unitn.it/>)
- [18] G. Oliveri, M. Donelli, and A. Massa, "Genetically-designed arbitrary length almost difference sets," *Electronics Lett.*, 2009, **5**, (23), pp. 1182-1183

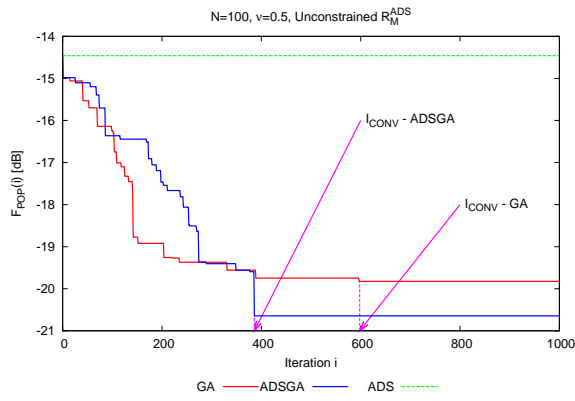
## FIGURE CAPTIONS

- **Figure 1.** *Problem I* ( $N_{ADS} = 100, \nu_{ADS} = 0.5$ ) - Synthesis results from the  $R_M$ -Unconstrained (*left column*) and  $R_M$ -Constrained (*right column*) approaches: (a)(b) behavior of the optimal fitness value,  $F_{POP}(i) = PSL(i)$ , versus the iteration number,  $i$ , (c)(d) power patterns plots,  $|S(u)|^2$ , and (e)(f) array arrangements.
- **Figure 2.** *Problem I* ( $N_{ADS} = 100, \nu_{ADS} = 0.5$ ) - Representative points in the space ( $U_M, PSL$ ) of the ADS-based arrays derived from the shifted versions of the (100, 50, 24, 25)-ADS [17].
- **Figure 3.** *Problem I* ( $\nu_{ADS} = 0.5$ ) - Synthesis results from the  $R_M$ -Unconstrained (I) and  $R_M$ -Constrained (II) approaches versus  $N$  (array dimension): (a) peak sidelobe level,  $PSL$ , (b) first null location,  $U_M$ , (c) convergence iteration number,  $I_{conv}$ , and (d) normalized array aperture,  $\frac{\Phi}{N}$ .
- **Figure 4.** *Problem I* ( $N_{ADS} = 198, \nu_{ADS} = 0.5$ ) - Synthesis results from the  $R_M$ -Unconstrained (*left column*) and  $R_M$ -Constrained (*right column*) approaches: (a)(b) power patterns plots,  $|S(u)|^2$ , and (c)(d) array arrangements.
- **Figure 5.** *Problem I* ( $N_{ADS} = 502, \nu_{ADS} = 0.5$ ) - Synthesis results from the  $R_M$ -Unconstrained (*left column*) and  $R_M$ -Constrained (*right column*) approaches: (a)(b) power patterns plots,  $|S(u)|^2$ , and (c)(d) array arrangements.
- **Figure 6.** *Problem II* ( $\hat{N} = 198, \hat{\nu} = 0.601$ ) - Synthesis results from the  $R_M$ -Unconstrained (*left column*) and  $R_M$ -Constrained (*right column*) approaches: (a)(b) behavior of the optimal fitness value,  $F_{POP}(i) = PSL(i)$ , versus the iteration number,  $i$ , (c)(d) power patterns plots,  $|S(u)|^2$ , and (e)(f) array arrangements with the ADSGA, the GA, and the ADS-based method.
- **Figure 7.** *Problem II* ( $\hat{N} = 200, \hat{\nu} = 0.77$ ) - (a) Behavior of the optimal fitness value,  $F_{POP}(i) = PSL(i)$ , versus the iteration number,  $i$ , (b) power patterns plots,  $|S(u)|^2$ , and (c) array arrangements with the ADSGA, the standard GA, the ADS-based method, and the solution in [5].

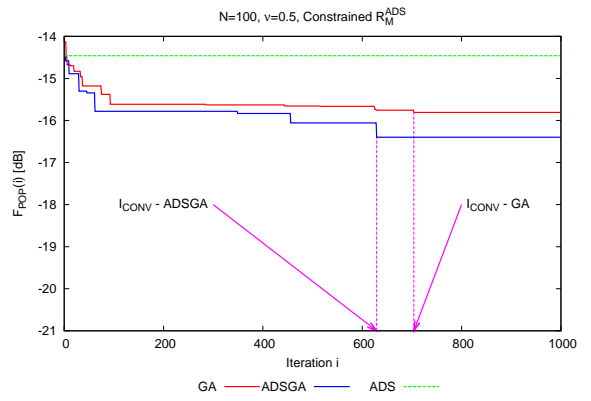
- **Figure 8.** *Problem II* - Representative points in the space  $(U_M, PSL)$  of the thinned arrays synthesized when  $\hat{N} = 198, \hat{\nu} = 0.601$  and  $\hat{N} = 200, \hat{\nu} = 0.77$ .
- **Figure 9.** *Problem III* ( $\hat{N} = 55$ ) - (a) Behavior of the optimal fitness,  $F_{POP}$ , versus the iteration number,  $i$ , and (b) three-level autocorrelation function of the convergence *ADS* arrangement (c).
- **Figure 10.** *Problem III* ( $\hat{N} = 214$ ) - (a) Behavior of the optimal fitness,  $F_{POP}$ , versus the iteration number,  $i$ , and (b) three-level autocorrelation function of the convergence *ADS* arrangement (c).
- **Figure 11.** *Problem III* - Plots of the power patterns and samples of  $\Xi(k)$  for the thinned arrangements from (a) the  $(55, 7, 0, 12)$ -*ADS* and (b) the  $(214, 10, 0, 123)$ -*ADS*.

## TABLE CAPTIONS

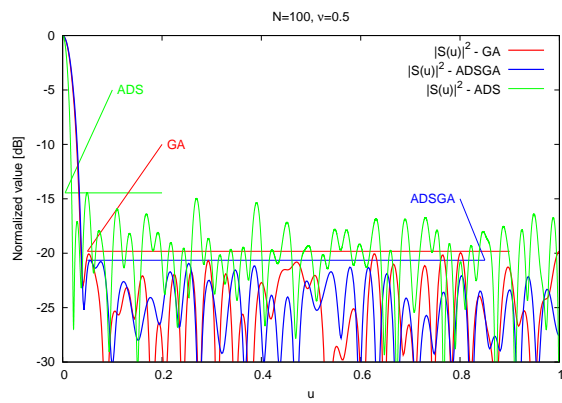
- **Table I.** *Problem I* ( $N_{ADS} = 100, \nu_{ADS} = 0.5$ ) - Comparative assessment.
- **Table II.** *Problem I* ( $N_{ADS} = 198, \nu_{ADS} = 0.5$ ) - Comparative assessment.
- **Table III.** *Problem I* ( $N_{ADS} = 502, \nu_{ADS} = 0.5$ ) - Comparative assessment.
- **Table IV.** *Problem II* ( $\hat{N} = 198, \hat{\nu} = 0.601$ ) - Comparative assessment.
- **Table V.** *Problem II* ( $\hat{N} = 200, \hat{\nu} = 0.77$ ) - Comparative assessment.



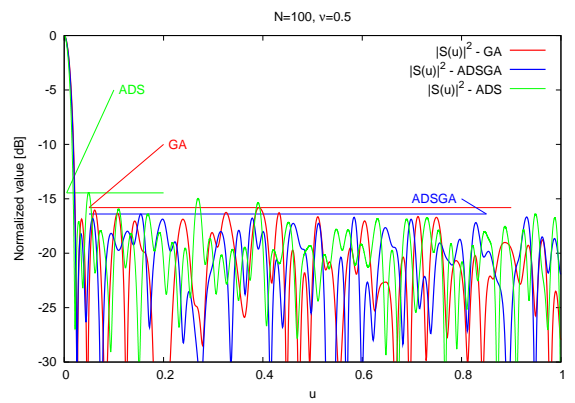
(a)



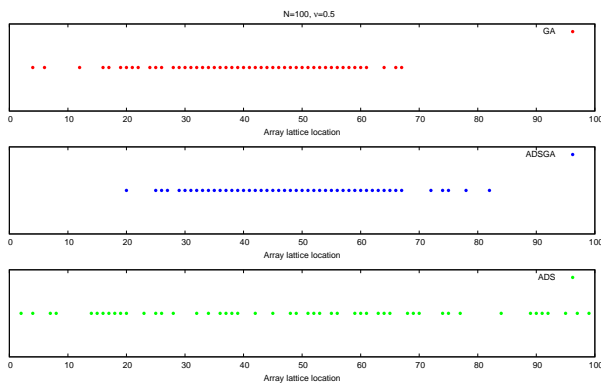
(b)



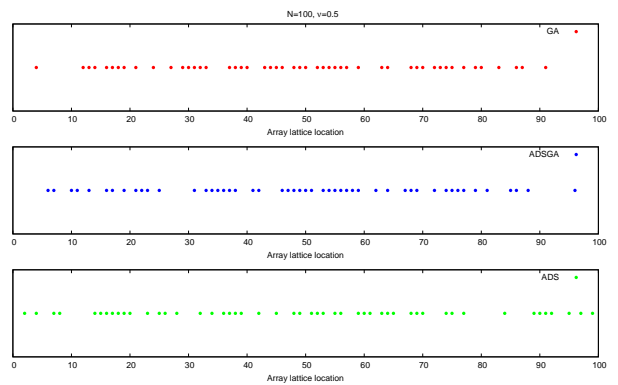
(c)



(d)



(e)



(f)

Figure 1 - G. Oliveri et al., "GA-Enhanced ADS-Based Approach for Array Thinning"

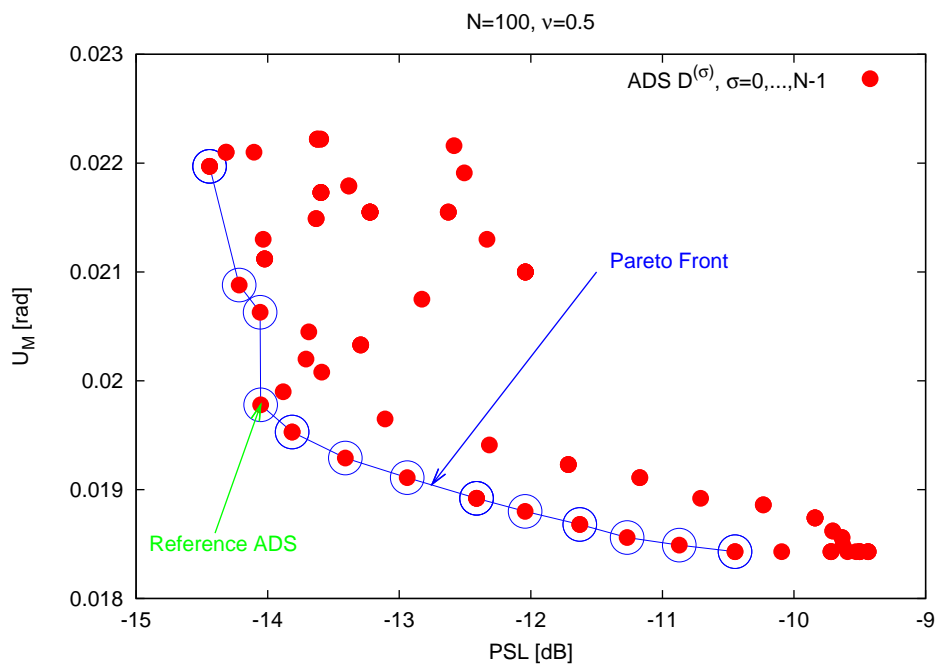
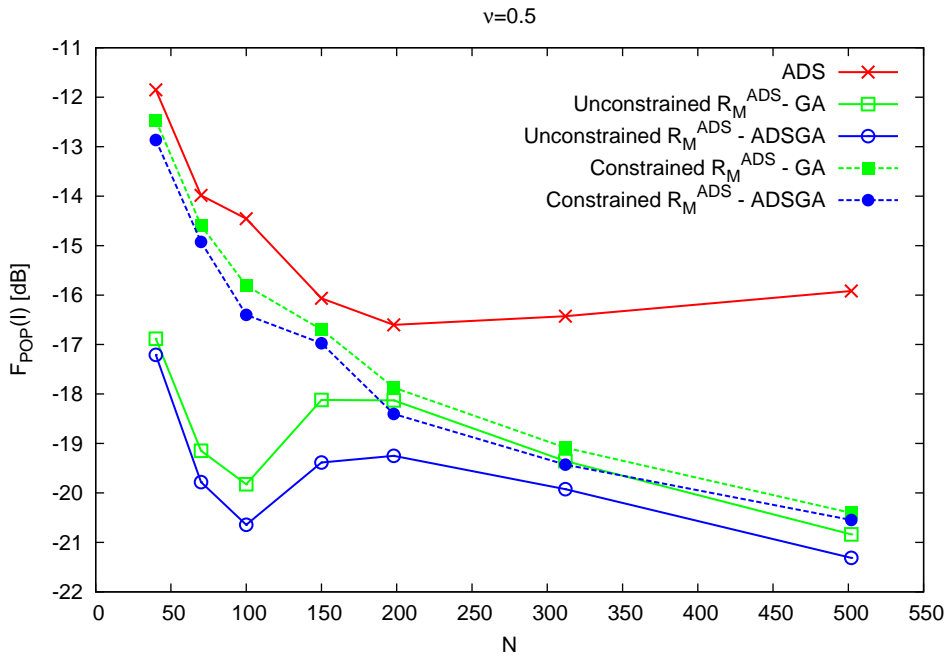
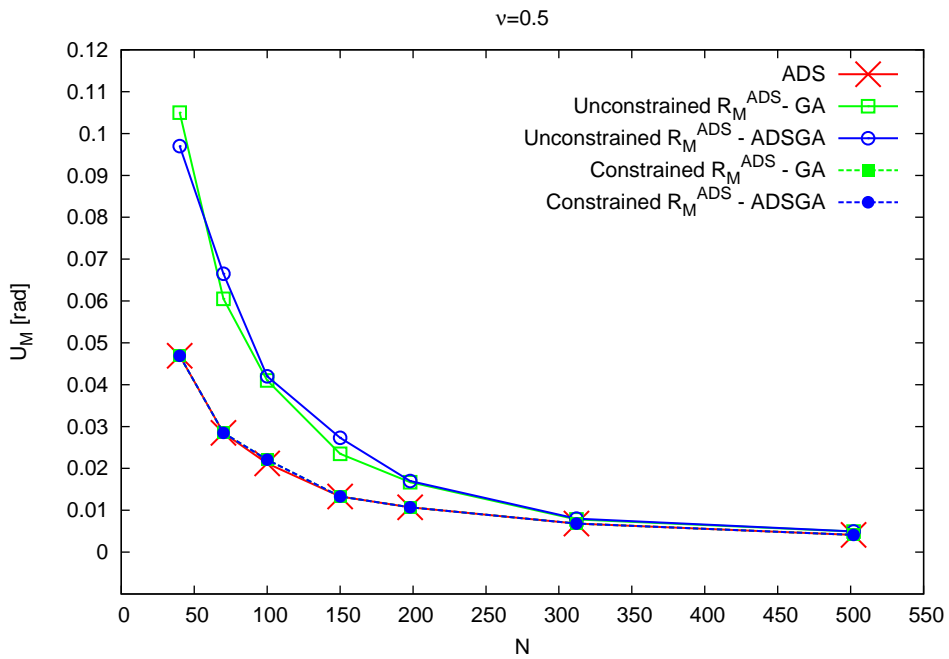


**Figure 2 - G. Oliveri et al., “GA-Enhanced ADS-Based Approach for Array Thinning”**

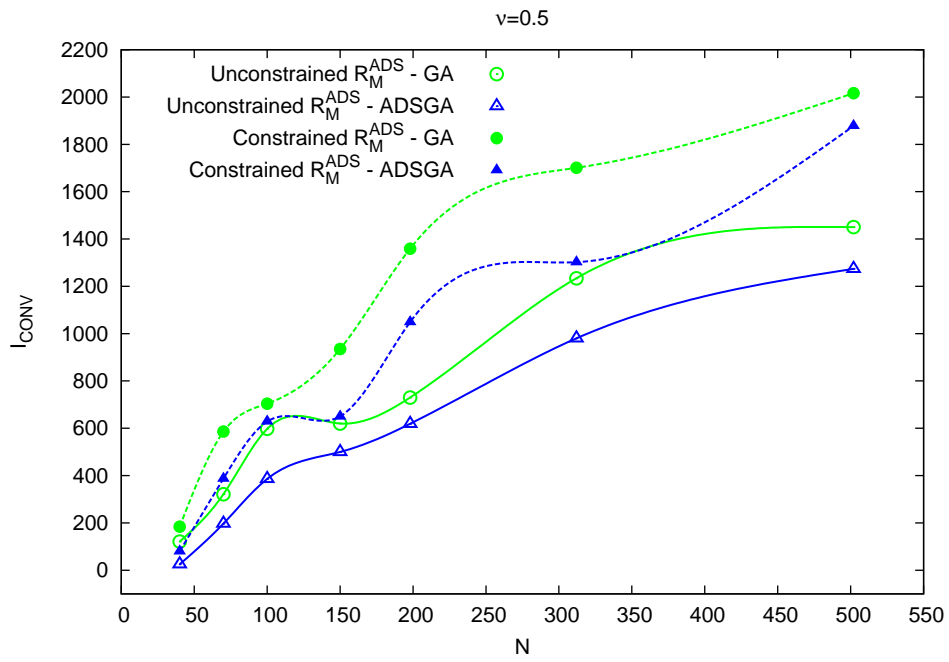


(a)

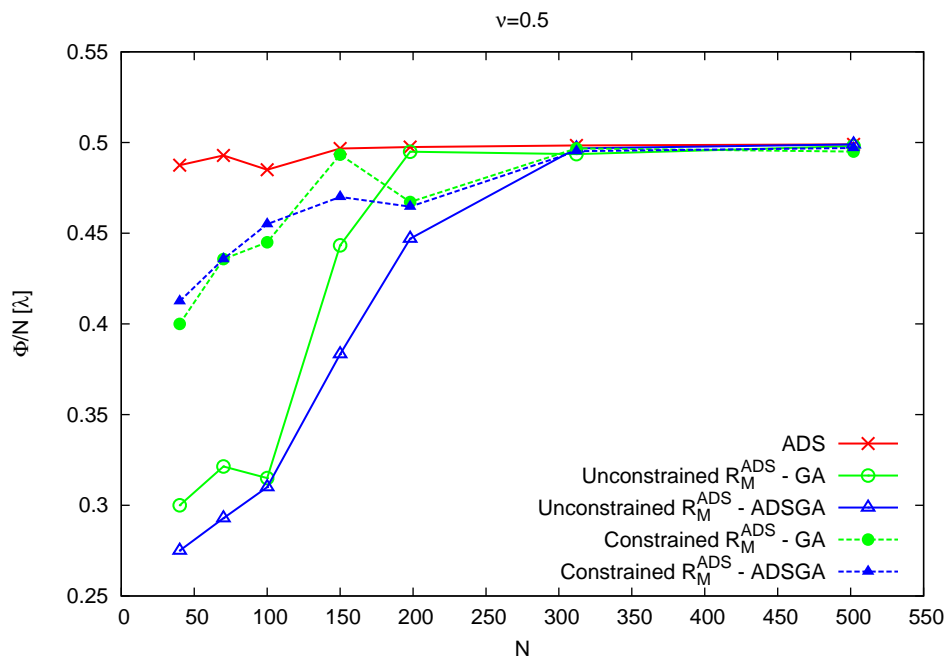


(b)

Figure 3(I) - G. Oliveri et al., "GA-Enhanced ADS-Based Approach for Array Thinning"

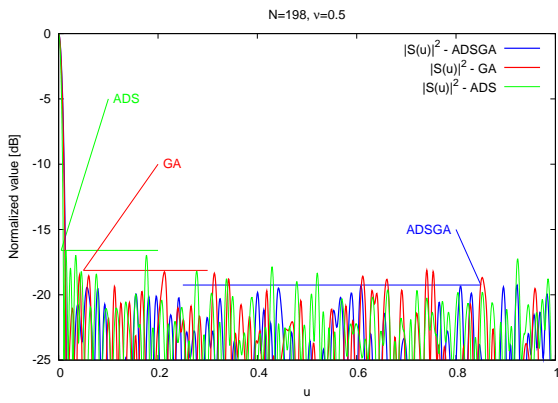


(c)

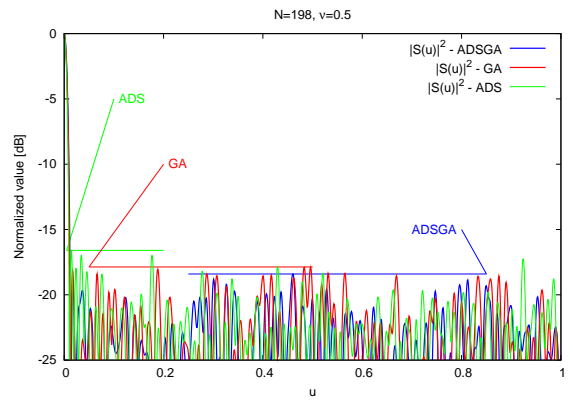


(d)

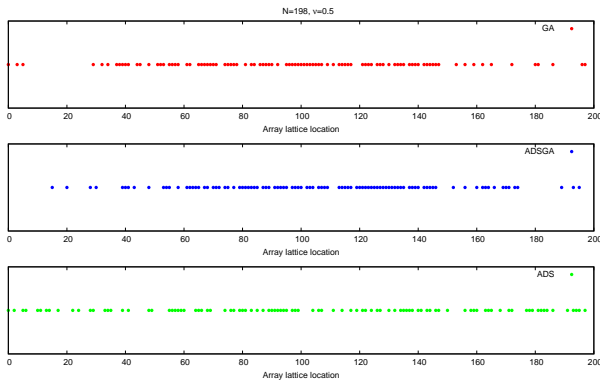
Figure 3(II) - G. Oliveri et al., "GA-Enhanced ADS-Based Approach for Array Thinning"



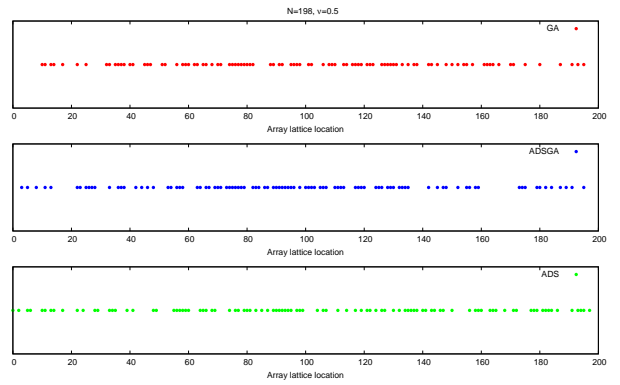
(a)



(b)

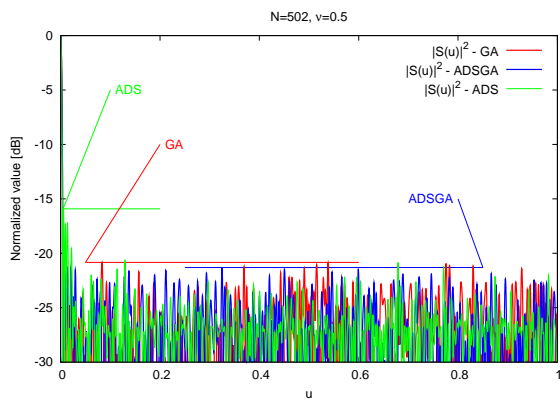


(c)

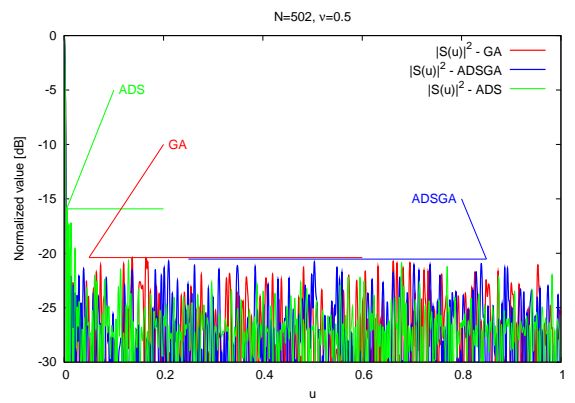


(d)

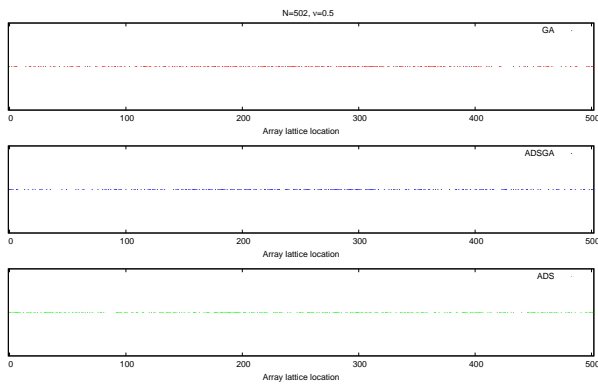
Figure 4 - G. Oliveri et al., "GA-Enhanced ADS-Based Approach for Array Thinning"



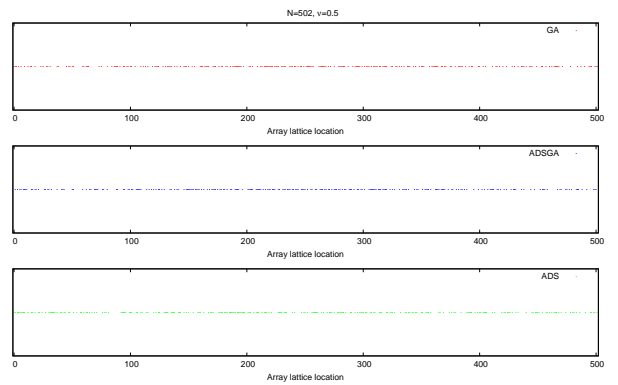
(a)



(a)

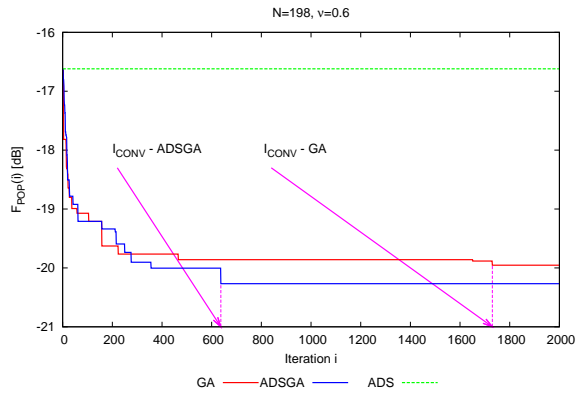


(b)

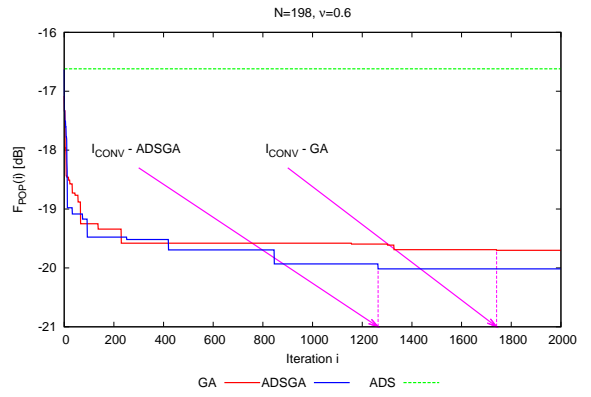


(b)

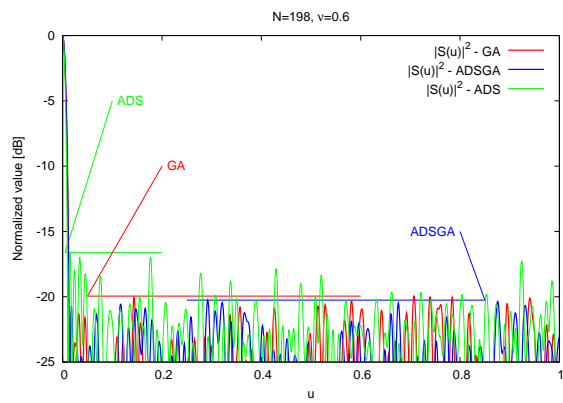
Figure 5 - G. Oliveri et al., "GA-Enhanced ADS-Based Approach for Array Thinning"



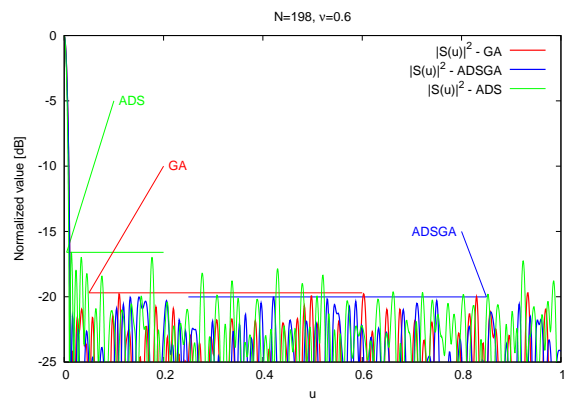
(a)



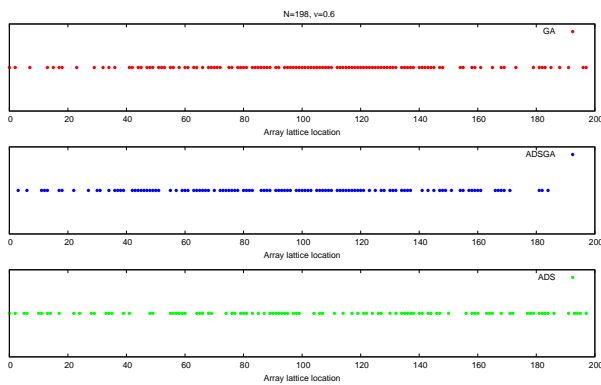
(b)



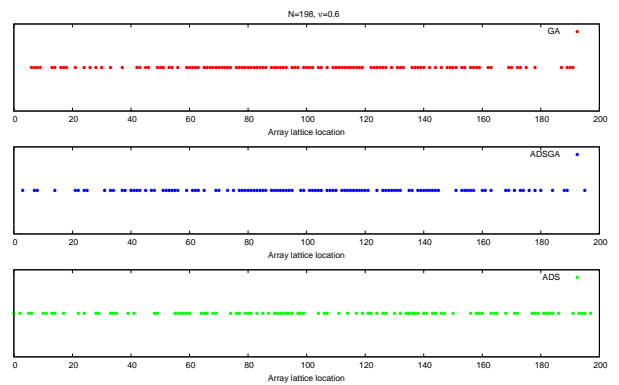
(c)



(d)

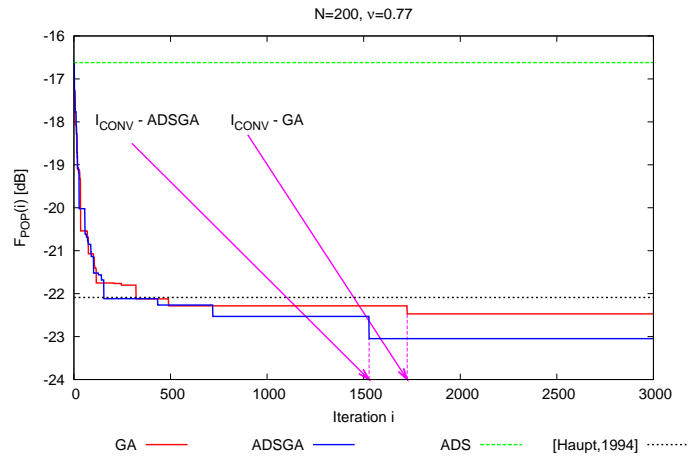


(e)

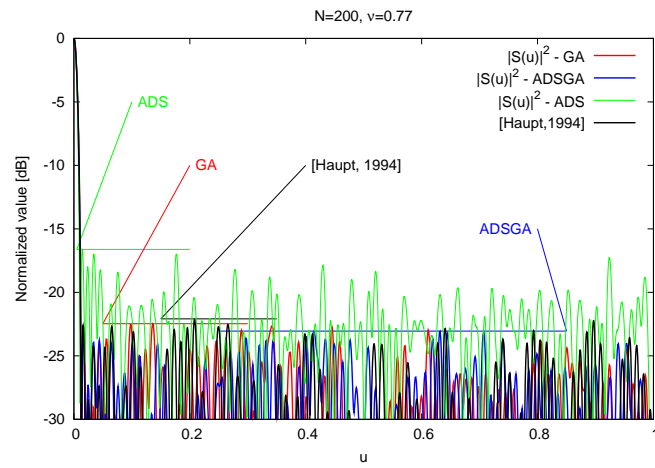


(f)

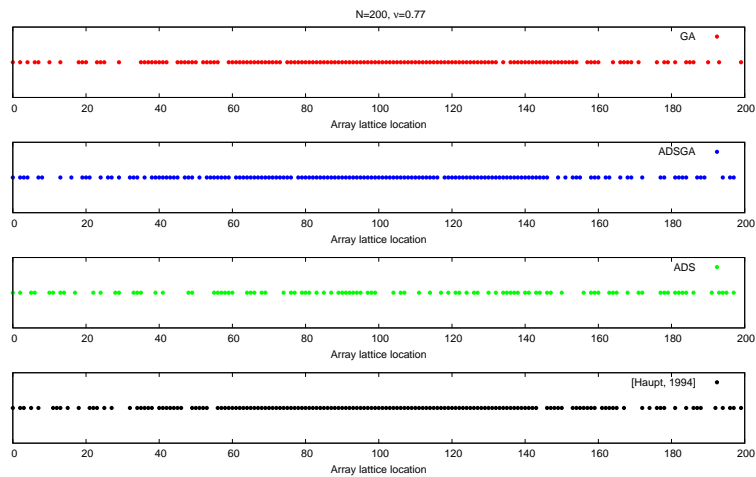
Figure 6 - G. Oliveri et al., "GA-Enhanced ADS-Based Approach for Array Thinning"



(a)



(b)



(c)

Figure 7 - G. Oliveri et al., "GA-Enhanced ADS-Based Approach for Array Thinning"

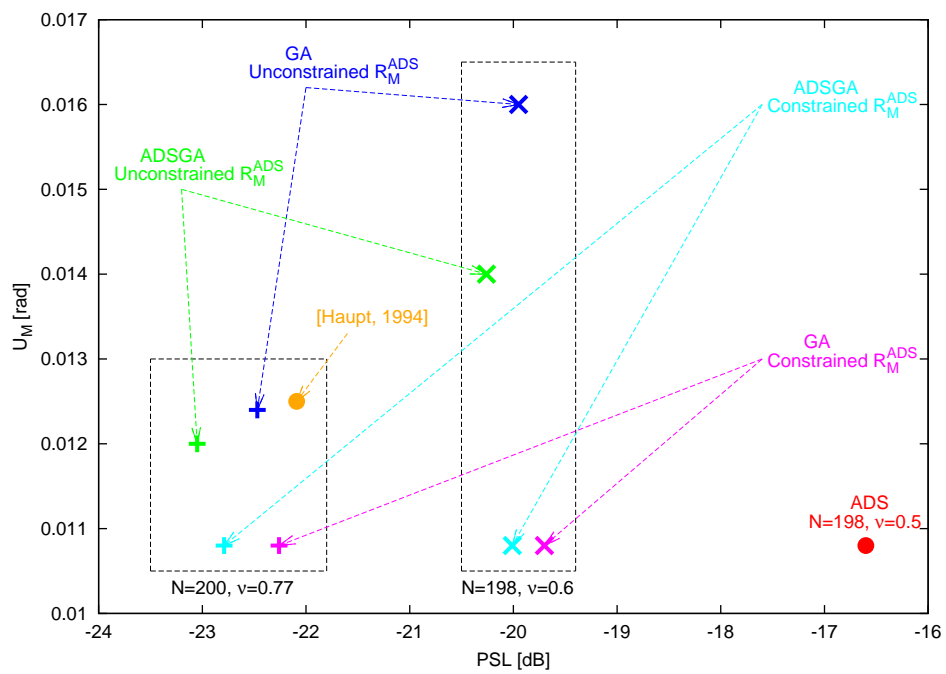
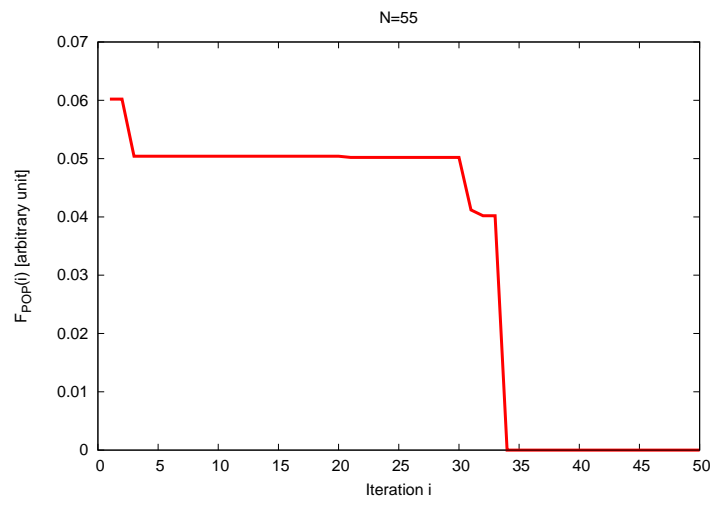
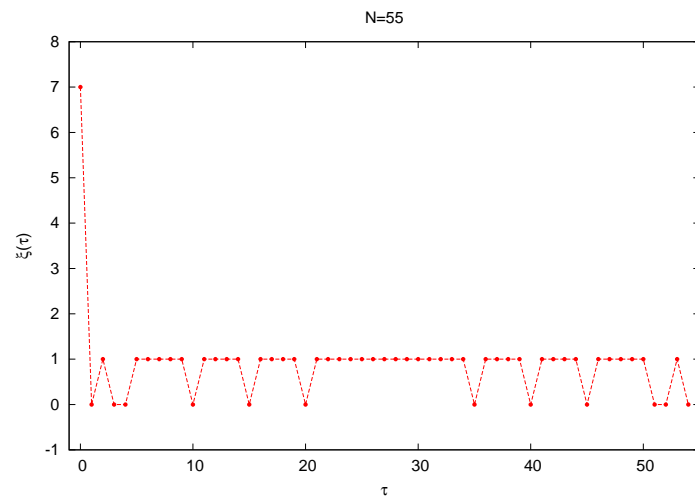


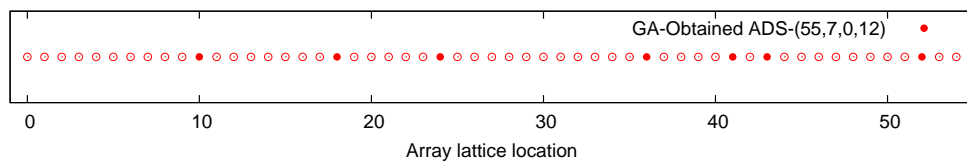
**Figure 8 - G. Oliveri et al., “GA-Enhanced ADS-Based Approach for Array Thinning”**



(a)

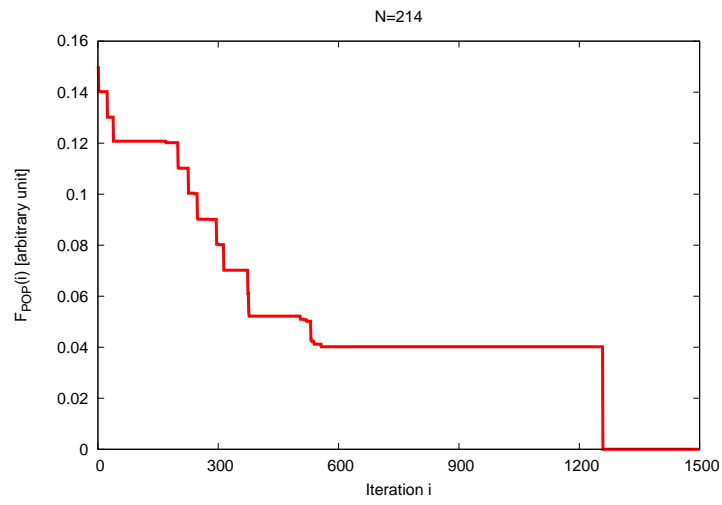


(b)

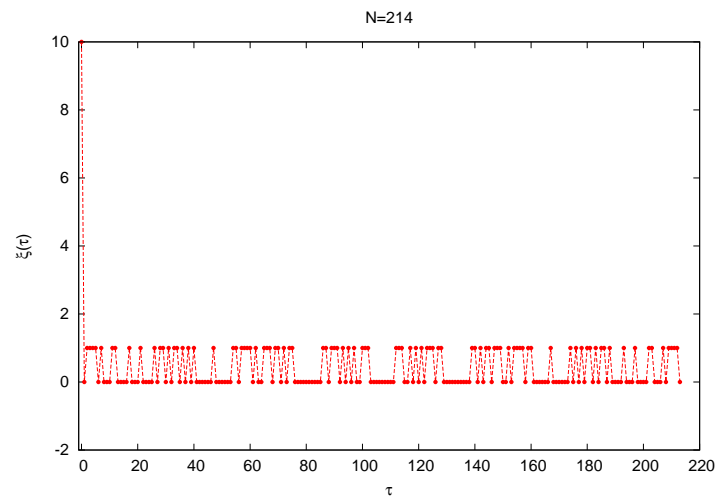


(c)

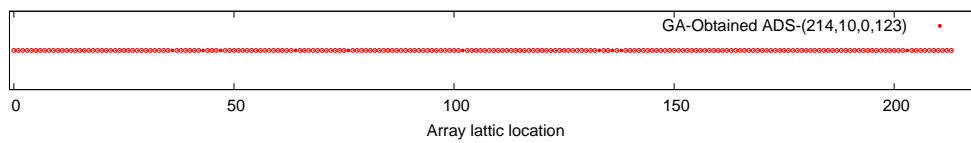
Figure 9 - G. Oliveri et al., “GA-Enhanced ADS-Based Approach for Array Thinning”



(a)

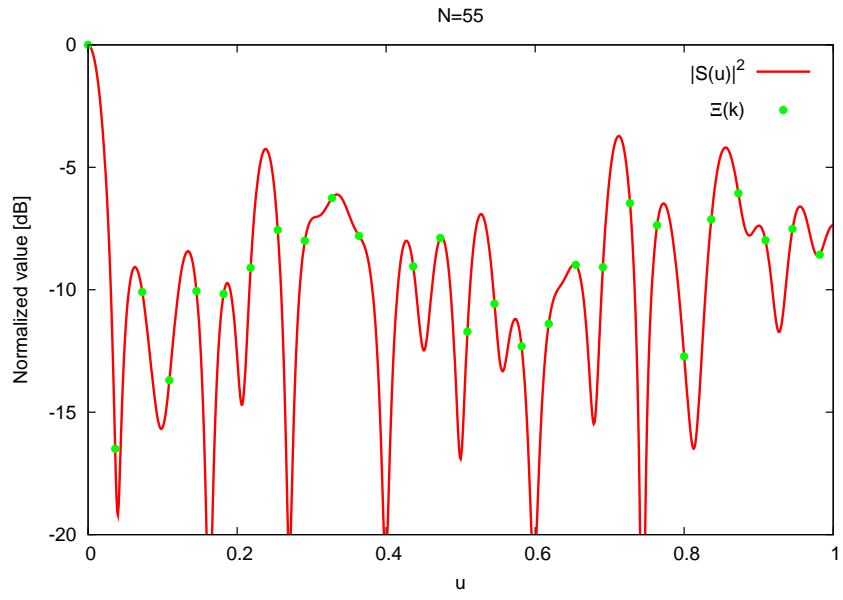


(b)

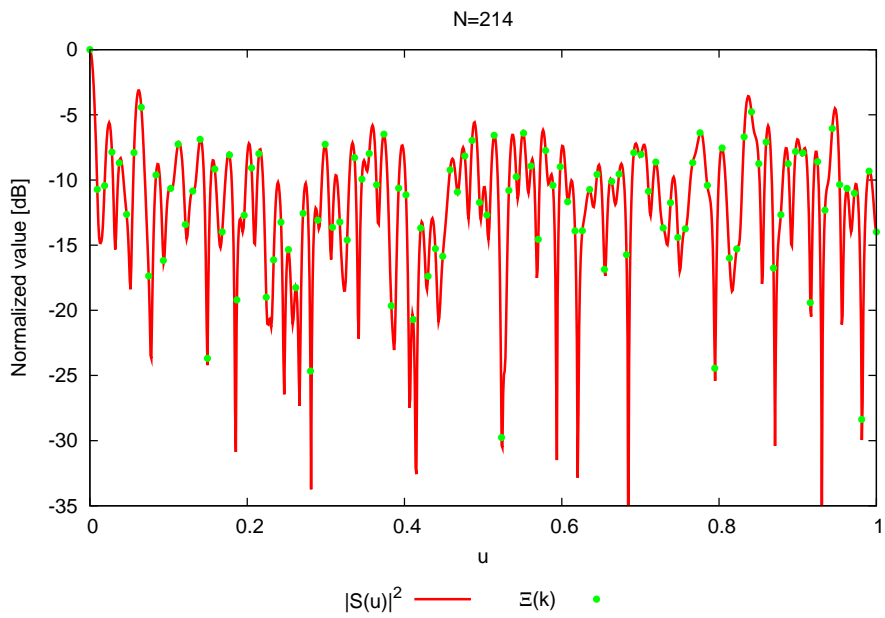


(c)

**Figure 10 - G. Oliveri et al., “GA-Enhanced ADS-Based Approach for Array Thinning”**



(a)



(b)

**Figure 11 - G. Oliveri et al., “GA-Enhanced ADS-Based Approach for Array Thinning”**

	<i>Unconstrained <math>R_M^{ADS}</math></i>			<i>Constrained <math>R_M^{ADS}</math></i>	
	<i>ADS</i>	<i>GA</i>	<i>ADSGA</i>	<i>GA</i>	<i>ADSGA</i>
$\Phi$ [ $\lambda$ ]	48.5	31.5	31	44.5	45.5
<i>Average spacing</i> [ $\lambda$ ]	0.989	0.642	0.632	0.908	0.928
<i>PSL</i> [dB]	-14.45	-19.82	-20.64	-15.71	-16.39
$U_M$ [rad]	0.020	0.041	0.041	0.022	0.022
$I_{CONV}$	-	598	386	704	629
<i>Average iteration time</i> [s]	-	0.397	0.397	0.397	0.397

**Table I - G. Oliveri et al., “GA-Enhanced ADS-Based Approach for Array Thinning”**

	<i>Unconstrained <math>R_M^{ADS}</math></i>			<i>Constrained <math>R_M^{ADS}</math></i>	
	<i>ADS</i>	<i>GA</i>	<i>ADSGA</i>	<i>GA</i>	<i>ADSGA</i>
$\Phi$ [ $\lambda$ ]	98.5	98	88.5	92.5	92.0
<i>Average spacing</i> [ $\lambda$ ]	1.005	1.000	0.903	0.943	0.938
<i>PSL</i> [dB]	-16.60	-18.12	-19.24	-17.86	-18.40
$U_M$ [rad]	0.0108	0.0167	0.0170	0.0108	0.0108
$I_{CONV}$	-	730	619	1359	1049
<i>Average iteration time</i> [s]	-	0.704	0.704	0.704	0.704

**Table II - G. Oliveri et al., “GA-Enhanced ADS-Based Approach for Array Thinning”**

		<i>Unconstrained</i> $R_M^{ADS}$		<i>Constrained</i> $R_M^{ADS}$	
		<i>ADS</i>	<i>GA</i>	<i>ADSGA</i>	<i>GA</i>
$\Phi$ [ $\lambda$ ]	250.5	250.0	250.5	248.5	249.5
<i>Average spacing</i> [ $\lambda$ ]	1.002	1.000	1.002	0.994	0.998
<i>PSL</i> [dB]	-15.91	-20.83	-21.31	-20.40	-20.54
$U_M$ [rad]	$4.12 \times 10^{-3}$	$4.90 \times 10^{-3}$	$4.93 \times 10^{-3}$	$4.12 \times 10^{-3}$	$4.12 \times 10^{-3}$
$I_{CONV}$	-	1450	1274	2000	1878
<i>Average iteration time</i> [s]	-	3.723	3.723	3.723	3.723

**Table III - G. Oliveri et al., “GA-Enhanced ADS-Based Approach for Array Thinning”**

		<i>Unconstrained <math>R_M^{ADS}</math></i>			<i>Constrained <math>R_M^{ADS}</math></i>	
	<i>ADS</i>	<i>GA</i>	<i>ADSGA</i>	<i>GA</i>	<i>ADSGA</i>	
$\Phi$ [ $\lambda$ ]	98.5	98.0	90.5	92.5	96.0	
<i>Average spacing</i> [ $\lambda$ ]	1.005	0.830	0.766	0.783	0.813	
<i>PSL</i> [dB]	-16.60	-19.95	-20.26	-19.70	-20.01	
$U_M$ [rad]	0.0108	0.0160	0.0140	0.0108	0.0108	
$I_{CONV}$	-	1730	637	1741	1264	
<i>Average iteration time</i> [s]	-	0.704	0.704	0.704	0.704	

**Table IV - G. Oliveri et al., “GA-Enhanced ADS-Based Approach for Array Thinning”**

		<i>Unconstrained <math>R_M^{ADS}</math></i>			<i>Constrained <math>R_M^{ADS}</math></i>		
	<i>ADS</i>	<i>GA</i>	<i>ADSGA</i>	<i>GA</i>	<i>ADSGA</i>	[5]	
$\Phi$ [ $\lambda$ ]	98.5	99.5	98.5	99.0	98.5	99.5	
<i>Average spacing</i> [ $\lambda$ ]	1.005	0.650	0.643	0.647	0.643	0.650	
<i>PSL</i> [dB]	-16.60	-22.47	-23.05	-22.26	-22.79	-22.09	
$U_M$ [rad]	0.0108	0.0124	0.0120	0.0108	0.0108	0.0125	
$I_{CONV}$	-	1725	1528	2187	2062	-	
<i>Average iteration time</i> [s]	-	0.704	0.704	0.704	0.704	-	

**Table V - G. Oliveri et al., “GA-Enhanced ADS-Based Approach for Array Thinning”**